ISSN 1392–1207. MECHANIKA. 2022 Volume 28(5): 364–368

The Theoretical Value for the Tip Radius of Cracks and Notches

Goksel SARACOGLU
Faculty of Aeronautics and Astronautics, Iskenderun Technical University, 31200 Iskenderun, Hatay Türkiye,
E-mail: goksel.saracoglu@iste.edu.tr

crossref http://dx.doi.org/10.5755/j02.mech.31338

1. Introduction

The determination of the critical fracture stresses of the materials is primarily to determine the fracture toughness. The transformation of a flaw into a micro and then macro-crack size in the material and reaching a level that may endanger safety is related to this concept.

Many fracture models have been developed to predict the critical fracture stresses of materials [1]. These methodologies are grouped into stress fracture [2-5], fracture mechanics [6-8], and progressive damage models [9-12]. Stress fracture models especially the Point-Stress Criterion (PSC) and the Area-Stress Criterion (ASC) are more widely used because of relative simplicity [13]. These two-parameter criteria indicate that the characteristic distance at which the tensile strength is reached from the tip of the notch or crack is a material property. The results of the experiments carried out later allowed these criteria to be modified as a three-parameter model. These criteria have been extended to include any laminate with a symmetrical structure using the anisotropic plate solution introduced by Lekhnitskii [2].

The Inherent Flaw Model (IFM) has been widely used in approaches based on Fracture Mechanics according to the above classification [8]. The model considers the high energy regions due to stress concentration at the crack or notch tips as additional crack length and is similar to the PSC due to its simplicity. But, all of these models are based on the characteristic distance and needs at least two mechanical test results.

The loss of properties of materials over time follows a certain mathematical path, independent of the influencing factor and material. This mathematical way is in the form of a decreasing exponential function. The Residual Property Model (RPM) is a different methodology in that it presents the loss of material property in its general form [14]. The model can give valid results up to a limit where linearity is no longer valid. However, to apply the model, two experimental points are needed as with the other methodologies mentioned above to predict the exact variation of mechanical properties of polymeric materials as a function of energy involved, regardless of the extent of the damage and/or the source of the damage.

This paper is important in terms of estimating critical fracture stresses of all crack length to width ratios a/W and tensile strength σ_0 based on only the data of one fracture test. While doing this, the complementary equation, not the alternative of the stress intensity factor (SIF) equation, was proposed in Fracture Mechanics. The fact that the method proposed in this study is simple and applicable to all flaws as well as the ability to detect critical fracture stresses of other defect rates and un-notch strengths from one test data makes it different from other methodologies positively. In this way, Irwin's Equation is considered in the load direction derived in the region close to the crack tip, a theoretical constant value was obtained for the crack tip radius. To assess the validation of this new methodology, five different cases from the literature were evaluated and compared with the PSC and the IFM.

2. The proposed method

In Fig. 1, there is a hyperbolic notch in a part subjected to stress in both directions. The tip radius of curvature of the notch is ρ. The coordinate system starts inside the endpoint by $r = \rho/2$. When ρ/a (a half the crack length) is small compared to one, the origin is very close to the focal point of the ellipse or hyperbola representing the surface of the crack. This field equation in the load direction is similar to that for a "mathematically sharp" plane crack [15].

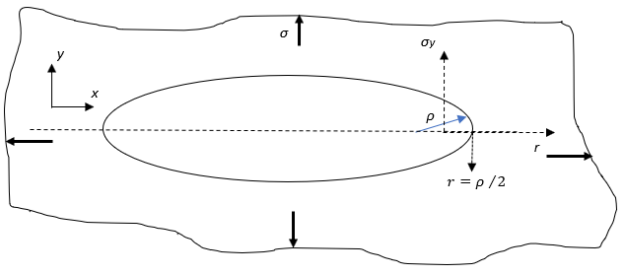

Fig. 1 Stress field coordinate system at hyperbolic notch tip [15]

The elastic stress distribution in the load direction adjacent to the elliptical holes and hyperbolic notches will be as in Eq. (1) [15]. K_I and σ_y represents the Mode-I SIF and the stress in the load direction at the notch tip.

$$\sigma_y = \frac{K_I}{(2\pi r)^{1/2}} \cos\frac{\theta}{2}\left[1+\sin\frac{\theta}{2}\sin\frac{3\theta}{2}\right]+ \\ +\frac{K_I}{(2\pi r)^{1/2}}\frac{\rho}{2r}\cos\frac{3\theta}{2}. \quad (1)$$

$\theta = 0°$ and $r = \rho/2$ should be used for the maximum stress in the load direction at the crack tip (Eq. (2)):

$$\sigma_{max} = 2K_I/(\pi\rho)^{1/2}. \quad (2)$$

If the theoretical tip curvature radius of 1.2732 mm is used for ρ in Eq. (2), the maximum stress (in MPa) in the direction of the load at the tip of the notch and the stress intensity factor (SIF, K_I) (in MPa.mm$^{1/2}$) will be equal to each other in value. Indeed, for crack propagation in a stressed specimen that contains cracks, the stress intensity

at the crack tip must reach fracture toughness. The value of the stress intensity achieved will be the same as the maximum stress that occurs in front of a notch with a tip radius of 1.2732 mm, which will be considered imaginary instead of this crack. So, using the theoretical value of ρ (1.2732 mm) for very small crack length ratios, Eq. (3) will be achieved at the limit of a/W=0. The σ_0 represents the tensile strength of the specimen:

$$K_I = \sigma_0 (\pi\rho)^{1/2}, (\rho = 1.2732 \text{ mm}). \quad (3)$$

In Linear Elastic Fracture Mechanics, SIF is stated by Eq. (4). The geometric correction factors Y for various test specimens are given in [16].

$$K_I = \sigma_f Y (\pi a)^{1/2}. \quad (4)$$

Regardless of the crack size, Eqs. (3) and (4) will give the same result for a material toughness. Thus, the ratio of critical fracture stress σ_f to tensile strength σ_0 will depend on constant theoretical tip radius σ_0, crack length a, and geometric correction factor Y as in Eq.5:

$$\frac{\sigma_f}{\sigma_0} = \frac{1}{Y}\left[\frac{\rho}{a}\right]^{1/2}, (\rho = 1.2732 \text{ mm}). \quad (5)$$

Eq. (5) will yield all the critical fracture stresses including approximate tensile strength with only single fracture test data of any kind of specimen. For the pin-loaded single-edge cracked tensile specimen, the geometric factor Y given in [16] is used as in Eq. (5). However, since the Y given in [16] is suitable for the pin-loaded condition, it should be used as $Y^{1/2}$ in Eq. (5) when used for clamped-end single-edge cracked specimen as seen in Eq. (6):

$$\frac{\sigma_f}{\sigma_0} = \left[\frac{\rho}{Ya}\right]^{1/2}, (\rho = 1.2732 \text{ mm}). \quad (6)$$

The propagation of the crack or notch is possible by reaching the material toughness value at the tip point. Therefore, at a theoretical tip radius of 1.2732 mm, the stress value (in MPa) that will occur at the tip will be the same as the toughness value (in MPa.mm$^{1/2}$). When ρ = 1.2732 mm value is entered in Eq. (1), the maximum principal stress distribution that will occur in front of the defect will be as in Eq. (7):

$$\sigma_y = \frac{K_I}{(2\pi r)^{1/2}}\left[1 + \frac{0.6366}{r}\right]. \quad (7)$$

It should be noted that in Eq. (7), the origin of r lies within 0.6366 mm of the theoretical crack or notch.

Not just cracks, circular holes can be solved similarly. The maximum stress that will occur at the edge of a hole of radius R (other than 1.2732 mm) in the specimen under the tensile stress will correspond to a certain ratio $\left[2/(\pi R)^{1/2}\right]$ of fracture toughness with respect to the value of radius R as in Eq. (8):

$$\sigma_{max} = \frac{2K_I}{(\pi R)^{1/2}} = K_t \sigma_f. \quad (8)$$

The σ_{max} is also the critical fracture stress σ_f multiplied by the stress concentration factor K_t. Therefore, it is indicated on the right-hand side of the Eq. (8).

The stress concentration K_t at the very small crack length emerging from the hole edge is given by Eq. (9) [17]:

$$K_t = 1 + 2\left[\frac{\rho}{a}\right]^{1/2}. \quad (9)$$

Since the theoretical ρ of 1.2732 mm is the equivalent of $4/\pi$, Eqs. (8) and (9) can be linked. As a result of this connection, Eq. (10) is reached:

$$K_t = 1 + \frac{4}{(\pi R)^{1/2}}. \quad (10)$$

If the stress concentration K_t is taken as in Eq. (10) and the stress intensity K_I is taken as in Eq. (3) and put in Eq. (8), σ_f/σ_0 is obtained as in Eq. (11):

$$\frac{\sigma_f}{\sigma_0} = \left[\frac{2(\pi\rho)^{1/2}}{4 + (\pi R)^{1/2}}\right]\frac{1}{Y^2}. \quad (11)$$

The factor Y in Eq. 11 is included to consider the effect of the specimen edge on the hole edge. The Y is the polynomial equation of the central crack specimen.

If the tensile strength σ_0 of the specimen including a circular hole is known, the critical fracture stress σ_f can be found with the help of Eq. (11), or vice versa.

3. Model verification

The proposed approach has been applied to $[0/90/\pm45]_{ns}$ Thornel T300 carbon fiber/epoxy laminated composite including cracks and holes with different test methods. The results of them examined in their studies [10, 18]. The σ_0, E_{11}, E_{22} and υ_{12} are 581 MPa, 138 GPa, 11 GPa and 0.35, respectively. The proposed method was compared with the results of the DZM, PSC and IFM as well as the experimental results.

The method has also been applied to [0/90] woven glass fiber/polyester laminated composite material for central cracked specimen [19]. The σ_0, E_{11}, E_{22} are 291 MPa, 7491 MPa and 6376 MPa, respectively.

The first specimen considered is the single-edge cracked tensile carbon fiber/epoxy laminated composite (SENT) specimen (Fig. 2, a) [18]. If the σ_0 (581 MPa) is used in Eq. (6), it is sufficient to enter the crack length a to determine the related σ_f. Eq. (5) was not used since the SENT specimen under consideration was tested with the clamped-end.

In Table 1, it is seen that the maximum deviation rate of the proposed method from the test results is 9.13%. It is also seen that the DZM, IFM and PSC are 9.3%, – 49.2% and –54.2%, respectively.

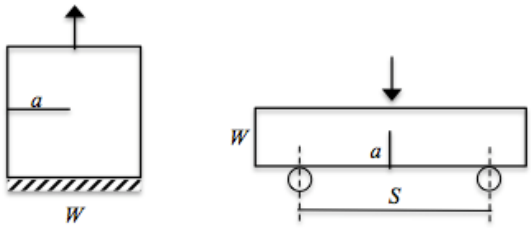

a b

Fig. 2 $[0/90/\pm45]_{ns}$ specimen: a) SENT; b) TPB schematic view

Table 1

SENT test results comparison (in MPa)

a/W	Exp.	DZM	IFM c_0=1.64 mm	PSC d_0=0.63 mm	This paper Eq. (6)
0.2	204	223	175	169	198
0.3	135	137	121	113	147
0.4	113	108	84	77	113
0.5	87	92	56	52	87
0.6	71	54	37	33	67

The second example is the three-point bending (TPB) carbon fiber/epoxy laminated composite specimen (Fig. 2, b) [18]. The other methodologies have determined the critical fracture stresses of other crack lengths by taking the critical fracture stress determined at a/W = 0.24 as reference. The same reference could be used for the proposed method. However, Table 2 is based on the tensile strength. It is seen that the proposed method gives very close results with the DZM and PSC.

Table 2

TPB test results comparison (in MPa)

a/W	Exp.	DZM	IFM c_0=1.64 mm	PSC d_0=0.63 mm	This paper Eq. (5)
0.24	269	269 (Ref.)			267
0.36	202	198	205	195	196
0.48	144	140	149	139	139
0.60	92	92	100	92	92
0.72	52	54	62	56	54

The third example is the compact tension (CT) specimen from the same material (Fig. 3, a) [18]. While the results close to the experimental results are obtained up to a/W = 0.45, it is seen that the deviation rate increases at larger a/W_s.

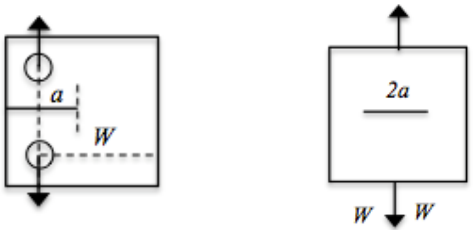

a b

Fig. 3 $[0/90/\pm45]_{ns}$ spec.: a) CT; b) CEN schematic view

The fourth example is the specimen with a central crack (CEN) specimen (Fig. 3, b). In [18], this specimen was fabricated from random glass fiber/polyester material. Although the proposed method gives results very close to the actual values at all a/W_s, the tensile strength found differs from the actual value since the fiber structure in the material does not show linear elastic characteristics. Therefore, in addition, a woven glass fiber/polyester material of a different study [19] is also included in Table 4. According to the ref. a/W =0.194, the tensile strength of the glass fiber/polyester laminated composite was determined as 277 MPa with an error rate of –4.8%.

Table 3

CT test results comparison (in MPa)

a/W	Exp.	DZM	IFM c_0=1.64 mm	PSC d_0=0.63 mm	This paper Eq. (6)
0.35	50	51	49	44	50
0.45	39	39	38	34	41
0.55	29	28	27	24	33
0.65	19	18	18	16	26

Table 4

CEN test results comparison (in MPa)

[18]			[19]			
a/W	Exp.	(Eq.5)	a/W	Exp.	(Eq. 5)	
0.0	135	205	0.000	291	Ref.	277
0.2	75 (Ref.)		0.194	127	133	Ref.
0.3	60	60	0.291	104	108	103
0.4	53	49	0.388	88	93	88
			0.485	77	82	78

The last two examples are related to the tensile specimens, which is produced from the same material but has the circular holes with a radius of 5 mm and 10 mm (Fig. 4) [10]. In the original study, by changing the width W on the W_0=140 mm plate, the critical fracture stress values in the plates containing the holes with 5 and 10 mm radii were determined.

Fig. 4 [0/90/±45] circular central hole spec. schematic view

Table 5

Predicted strengths for specimens with R=5 mm circular holes of various ratios W/W_0 (in MPa)

W/W_0	Exp.	DZM	IFM c_0=1.64 mm	This paper Eq. (10)
1.	284	288	301	291
2/3	290	286	294	290
1/2	285	282	286	288
1/3	276	268	263	284
1/4	267	253	247	264
1/5	237	236	229	248
1/7	206	195	183	207

When the proposed method is used, critical fracture stresses were determined with an error margin of +4.6% to –2.9%. The DZM has deviation rates of +1.4% to –5.3%, and the IFM has the range of +6% to –11.2% as seen in Table 5.

The critical fracture stresses obtained when the hole radius is increased to 10 mm are shown in Table 6. It is seen that the proposed method has the satisfactory deviation rates (max. –3.95%) according to the experimental results. It is also seen that the DZM and the IFM have deviation rates of –7.7% and –7.9%, respectively.

Table 6

Predicted strengths for specimens with R=10 mm circular holes of various ratios W/W_0 (in MPa)

W/W_0	Exp.	DZM	IFM c_0=1.64 mm	This paper Eq. (10)
1.	242	243	241	236
2/3	236	226	222	229
1/2	228	212	210	219
1/3	190	184	178	190
1/4	156	144	145	151

4. Conclusions

In this study, a simple approach is proposed that can be applied to all test kind samples whether the defect in the material is a sharp-edged crack or a hole with a certain radius. By generating an additional equation to the SIF of the Classical Fracture Mechanics, it is possible to determine the values of the other crack length ratios from one critical fracture stress. Using the two equations together also provides the tensile strength to be found from only one critical fracture stress value. The other methodologies put forward in this regard, on the other hand, can provide the determination of all values by using at least two data (e.g., tensile strength and a critical fracture stress) [1]. Fracture occurs when the stress intensity factor at the tip of the defect reaches the fracture toughness of the material. The use of the theoretical tip radius value, which will allow the value of the fracture toughness in MPA.mm$^{1/2}$ to be equal to the maximum stress in MPa, has brought an easy approach and has provided values close to the experimental results in many test methods.

In order for the method to be successful, the material must show linear elastic characteristics from a certain crack length ratio to the a/W=0 limit point.

Declarations

Funding. The author declares that there is no financial support of any foundation for this work.

Conflict of interest/Competing interests. The author declares that he has no known competing financial interests or personal relationships that could have appeared to influence the work reported in this paper.

References

1. **Awerbuch, J.; Madhukar, M. S.** 1985. Notched strength of composite laminates: predictions and experiments – a review, Journal of Reinforced Plastics and Composites. https://doi.org/10.1177/073168448500400102.
2. **Whitney, J. M.; Nuismer, R. J.** 1974. Stress fracture criteria for laminated composites containing stress concentrations, Journal of Composite Materials 8: 253-265. https://doi.org/10.1177/002199837400800303.
3. **Karlak, R. F.** 1977. Hole effects in a related series of symmetrical laminates. proceedings of failure modes in composites iV, The Metallurgical Society of AIME, Chicago, pp. 106−117.
4. **Pipes, R. B.; Wetherhold, R. C.; Gillespie, J. W.** 1979. Notched strength of composite materials, Journal of Composite Materials 13: 148 - 160. https://doi.org/10.1177%2F002199837901300206.
5. **Tan, S. C.** 1987. Notched strength prediction and design of laminated composites under in-plane loadings, Journal of Composite Materials 21: 750 - 780. https://doi.org/10.1177%2F002199838702100804.
6. **Tan, S. C.** 1988. Finite-width correction factors for anisotropic plate containing a central opening, Journal of Composite Materials 22: 1080 - 1097. https://doi.org/10.1177%2F002199838802201105.
7. **Gillespie, J. W.; Carlsson, L.** 1988. Influence of finite width on notched laminate strength predictions, Composites Science and Technology 32: 15-30. https://doi.org/10.1016/0266-3538(88)90027-9.
8. **Waddoups, M. E.; Eisenmann, J. R.; Kaminski, B. E.** 1971. Macroscopic fracture mechanics of advanced composite materials, Journal of Composite Materials 5: 446 - 454. https://doi.org/10.1177/002199837100500402.
9. **Mar, J. W.; Lin, K. Y.** 1977. Fracture mechanics correlation for tensile failure of filamentary composites with holes, Journal of Aircraft 14: 703-704. https://doi.org/10.2514/3.44618.
10. **Backlund, J. C.; Aronsson, C.** 1986. Tensile fracture of laminates with holes, Journal of Composite Materials 20: 259 - 286. https://doi.org/10.1177%2F002199838602000304.
11. **Chang, F. K.; Chang, K.** 1987. A progressive damage model for laminated composites containing stress concentrations, Journal of Composite Materials 21: 834 - 855. https://doi.org/10.1177%2F002199838702100904.
12. **Tan, S. C.** 1991. A progressive failure model for composite laminates containing openings, Journal of Composite Materials 25: 556 - 577. https://doi.org/10.1177%2F002199839102500505.
13. **Tsai, K. H.; Hwan, C.; Lin, M. J.; Huang, Y. S.** 2012. Finite element based point stress criterion for predicting the notched strengths of composite plates, Journal of Mechanics 28: 401-406. https://doi.org/10.1017/jmech.2012.48.
14. **Papanicolaou, G. C.; Kosmidou, T.; Vatalis, A. S.; Delides, C. G.** 2006. Water absorption mechanism and some anomalous effects on the mechanical and viscoelastic behavior of an epoxy system, Journal of Applied Polymer Science 99*:* 1328-1339. https://doi.org/10.1002/app.22095.

15. **Creager, M.; Paris, P.** 1967. Elastic field equations for blunt cracks with reference to stress corrosion cracking, International Journal of Fracture Mechanics 3: 247-252. https://doi.org/10.1007/BF00182890.
16. **Tada, H.; Paris, P. C.; Irwin, G. R.** 2000. The Stress Analysis of Cracks Handbook, Third Edition. ASME Press, New York. https://doi.org/10.1115/1.801535
17. **Pilkey, W.; Pilkey, D.** 2008. Peterson's stress concentration factors. Third edition. John Wiley & Sons, Inc., Hoboken, New Jersey. https://doi.org/10.1002/9780470211106
18. **Aronsson, C.; Backlund, J. C.** 1986. Tensile fracture of laminates with cracks, Journal of Composite Materials 20: 287 - 307. https://doi.org/10.1177/002199838602000305
19. **Khashaba, U. A.** 2003. Fracture behavior of woven composites containing various cracks geometry, Journal of Composite Materials 37: 20 - 5. https://doi.org/10.1177%2F0021998303037001679.

G. Saracoglu

THE THEORETICAL VALUE FOR THE TIP RADIUS OF CRACKS AND NOTCHES

S u m m a r y

In this paper, an additional equation that can be used in conjunction with the Stress Intensity Factor is produced, enabling the determination of all critical fracture stresses, including tensile strength, from only one mechanical test data. In this context, the blind elliptical hole stress distribution area equation of Creager and Paris was used and the theoretical radius value was selected to ensure that the maximum principal stress (in MPa) at the tip point and the fracture toughness (in $MPa.mm^{1/2}$) were equal in value. By using the obtained equation together with the stress intensity factor, the results very close to the experimental data were obtained in the test specimens with cracks and holes, regardless of the true radius of the crack tip.

Keywords: critical fracture stress; the residual property model; fracture stress predicting method; the stress distribution.

Received May 09, 2022
Accepted October 17, 2022